AAEC/E185

AAEC/E185

AUSTRALIAN ATOMIC ENERGY COMMISSION

RESEARCH ESTABLISHMENT

LUCAS HEIGHTS

THE EFFECTS OF IRRADIATION ON BERYLLIA BASED FUELS

by

B.S. HICKMAN
W.B. ROTSEY
R.J. HILDITCH
K. VEEVERS

September 1967

AUSTRALIAN ATOMIC ENERGY COMMISSION

RESEARCH ESTABLISHMENT

LUCAS HEIGHTS

THE EFFECTS OF IRRADIATION ON BERYLLIA BASED FUELS

by

B. S. HICKMAN
W. B. ROTSEY
R. J. HILDITCH
K. VEEVERS

ABSTRACT

Dispersions of $(UTh)O_2$ in beryllia, containing 1.7 per cent to 25 per cent $(UTh)O_2$ in three fuel particle sizes, coarse (150–200μ), medium (33–35μ) and fine ($<$10 and $\leq$5μ) were irradiated to burnups of 3–10 per cent of heavy metal atoms in the range 300–900 °C, in both fast and thermal fluxes. Changes in volume, lattice parameter, line breadth, and modulus of rupture were measured. Volume changes in the fine dispersions were ascribed wholly to fission fragment damage and were about 50 per cent greater than those caused by fast neutrons alone; they increased with increasing fission fragment flux, and decreased as irradiation temperature increased. Volume changes in medium and coarse dispersions were about 25 per cent greater than those caused by fast neutrons alone; the enhancement of the damage is attributed to the additional β flux. As fuel particle size increased, deterioration in strength under irradiation was more marked. This was attributed to more intense fission fragment damage in the recoil zone around larger particles causing volume increases which exceeded those of the remainder of the matrix. For maximum initial strength and retention of strength under irradiation the fuel particle size should not exceed 5μ, and the inter-particle spacing should not exceed 30μ.

CONTENTS

(continued)

CONTENTS (continued)

1. INTRODUCTION

Irradiation of dispersions of UO_2 or $(UTh)O_2$ in beryllia have led to some uncertainty in the design and performance of beryllia based dispersion fuels. Hanna et al. (1964) irradiated both coarse ($\sim 200\mu$ fuel particles) and fine ($<20\mu$ fuel particles) dispersions in a thermal flux in the A.A.E.C.'s reactor HIFAR and although from theory it was expected that the coarse dispersions would be superior, he found that the fine dispersions gave the better performance. In later work, Hanna and Hilditch (1965) found that fine dispersions retained strength as well as and possibly better than coarse dispersions. On the other hand, Mills et al. (1964) who irradiated 70 vol. per cent BeO – 30 vol. per cent UO_2 to burnups of 55 per cent of heavy metal atoms at temperatures up to 1100 °C, found that although coarse dispersions showed no gross cracks or deformation, all the fine dispersions broke into several pieces. In addition Hamner et al. (1964) irradiated 70 vol. per cent BeO – 30 vol. per cent UO_2 coarse dispersions at 1100 °C to a burnup of 1.6 per cent of heavy metal atoms and found that most specimens contained macrocracks, which were believed to originate from stresses set up on cooling after thermal stresses had been relaxed at high temperatures.

The present work was therefore undertaken to:

(a) investigate the effect of fuel particle size on irradiation behaviour,

(b) obtain reliable data on the mechanical properties of irradiated dispersions,

(c) determine the effect of both thermal and fast neutron dose on the properties,

and generally to establish the ground rules for the design of BeO dispersion fuels with maximum irradiation resistance.

2. EXPERIMENTAL DETAILS

2.1 Preparation of Materials

Thoria Particles: Thoria particles were prepared by calcining thorium oxide at 900 °C in air; the product was isostatically pressed at 20 t.s.i., crushed, sieved and finally sintered at 1700 °C for 3 hours in hydrogen.

Solid Solution $(UTh)O_2$ Particles: A mixture of ammonium di-uranate and $Th(OH)_2$ in the required proportions, was coprecipitated from a solution of the nitrates. The coprecipitated sludge was dried at about 85 °C for 24 hours. The dried powder was crushed to 85 mesh, reduced at 700 °C in hydrogen, and ground for 4 hours with beryllia balls. The product was pressed at 20 t.s.i., crushed and graded (−60 + 85 mesh) and sintered for 2 hours at 1700 °C in flowing hydrogen. The sintered product was then regraded to the required size fraction. The particles were contaminated with about 10 vol. per cent of beryllia during the milling operation, and contained trace impurities of nickel, chromium, and fluorine, with larger quantities of iron.

Beryllia: Brush UOX powder was homogenised by grinding for 1 hour in water with beryllia balls, sieved, filtered, and dried.

Dispersions in Beryllia: The heavy metal particles were dispersed in an alcohol slurry with beryllia, and the mixture dried. The resulting powder was isostatically pressed at 20 t.s.i. and sintered at 1500 °C for 1½ hours in nitrogen. In the final sintered dispersion, the particles were rounded but irregular in shape, and contained about 5 per cent finely distributed porosity. The grain size of the beryllia matrix was generally less than 5μ. Occasional areas of coarser grains were observed adjacent to particles, but in the $<5\mu$ dispersions the overall grain size was slightly coarser ($\sim 8\mu$), probably due to iron contamination. The several types of dispersions fabricated are listed in Table 1. Typical microstructures are shown in Figure 1. Materials A, B, C, D, and E were machined to 2.54 cm x 0.41 cm diameter, and annealed for 1 hour at 1000 °C in air to heal surface microcracks (Rotsey et al. 1967). Materials F and G were machined to 2 cm x 0.9 cm diameter, Material H to 1.5 x 0.75 cm diameter and Material J to 2.0 cm x 0.75 cm diameter.

2.2 Irradiation Details

Specimens were irradiated in graphite carriers in stainless steel cans. Temperatures, measured with chromel-alumel thermocouples, were controlled by manual variation of the composition of a helium-nitrogen mixture in a gas gap between the specimen can and an outer stainless steel can. Variations of up to 250 °C occurred, particularly in the early stages of the irradiation (Figure 2). Time weighted mean temperatures calculated from the temperature graphs are used in this report to indicate the mean irradiation temperature.

Integrated thermal and fast neutron fluxes in the various cans were obtained from cobalt and titanium flux monitor data and from previously measured flux levels in the reactor positions, (see Tables 2 and 3).

In the irradiation experiments the materials were divided into two groups. Group 1 comprised Materials F, G, H, and J which were irradiated by thermal neutrons. Two cylinders of each material at each temperature were irradiated. Group 2 comprised Materials A, B, C, D, and E which were irradiated with both thermal and fast neutrons; ten bend test specimens of each material at each temperature were irradiated.

3. RESULTS

3.1 Macroexamination

Post irradiation examination of the bend test specimens (Group 2) irradiated in a fast flux showed the following:

Material A : Of the 119 specimens irradiated, 2 were broken in half, and a further 15 of the 30 irradiated at 300 °C were extensively microcracked.

Material B : 9 of the 60 specimens were broken in half.

Material C : Only 1 out of the 59 was broken in half.

Material D : 2 out of 28 were broken in half.

Material E : All 59 specimens were sound.

In general, the condition of the specimens was excellent; breaks in 14 of the 325 were probably due to handling damage but the 15 extensively cracked after 300 °C irradiation were genuine test failures.

Examination of the specimens from Group 1 irradiated in a thermal flux revealed that only five were free from macrocracking, some were broken into two pieces, and the worst one was broken into six pieces. The calculated thermal stresses in these specimens ranged from 5,500 p.s.i. to 33,000 p.s.i., and the cracking was found to be closely related to the thermal stress; those with the lower thermal stresses did not crack, and the cracking became progressively worse as the thermal stress increased.

3.2 Dimensional Changes

Dimensional changes were measured on all specimens using a micrometer. The length changes in the bend test specimens (Group 2) were considered to be the most reliable measure of volume changes. Diameter changes were of much lower accuracy but within limits of measurement were of the same order as the length changes. The volume changes calculated are given in Tables 2 and 3, with estimated accuracy ± 20 per cent.

To confirm these results, density changes were measured before and after irradiation by displacement after vacuum impregnation with n-octyl alcohol. The results from Materials A and B (coarse fuel particles) showed a wide scatter of positive and negative changes. With the known dimensional changes this can only be attributed to increases in open porosity giving rise to higher

impregnated densities (the open porosity of all materials prior to irradiation was very low (<0.5 per cent)). However, Materials C to J inclusive gave changes in impregnated density of the same order as the density changes calculated from the dimensions, except where macro-cracking was extensive. This indicates that the open porosities of these specimens did not alter significantly with irradiation.

3.3 X-Ray Diffraction Studies

X-ray diffraction studies of the beryllia matrix from coarse, medium and fine dispersions are discussed in detail by Walker and Hickman (1967). Two important conclusions drawn were:

(a) The change in the c lattice parameter of coarse dispersions (Materials A and B) was much larger than unfuelled beryllia specimens irradiated alongside the fuel specimens. Typical examples are shown in Table 4.

(b) The change in the c lattice parameter of all fine dispersions was negligibly small.

3.4 Metallographic Examination

Specimens were prepared for metallographic examination by slitting, grinding on papers, and final polishing on a vibratory polishing machine using a medium grade alumina polishing powder. At least one specimen of each type from each can was examined.

(i) In Group 2, the presence of macrocracks in Material A irradiated at 300 °C, seen in the macroexamination at magnifications x4 to x13, was confirmed. The micro-examination however, revealed that macrocracks were present in all the coarse dispersions (see Figure 3) except those irradiated at the highest temperature of 875 °C. No macrocracks were found in the medium or fine dispersions.

(ii) Little or no cracking attributable to irradiation was observed in the fuel particles.

(iii) Considerable changes in the nature and distribution of the porosity occurred in the fuel particles. At burnups of around 5 per cent the amount of porosity decreased and this became more marked at higher irradiation temperatures. In Material D, at burnups of 12–14 per cent the number of large pores increased with increasing temperature.

(iv) In Group 1 specimens a diffuse fuel particle-matrix boundary was associated with the higher irradiation temperatures and higher burnups, see Figure 4.

3.5 Mechanical Testing

Modulus of rupture tests were made in air using four point bending with a gauge length of 1.09 cm and a span of 1.51 cm. After irradiation, material was tested at room temperature, and, where numbers permitted, at elevated temperatures, provided the irradiation temperature was not exceeded. Where possible ten specimens were tested in each condition. Pre-irradiation results were reported by Veevers and Rotsey (1966a) and post-irradiation results were reported briefly by Hilditch et al. (1966). Both sets of data are compared in Table 5. The pre-irradiation and the post-irradiation results both showed no significant variation in strength over the range 20–500 °C so the mean strengths over this range are given.

Some trends are clearly shown by Table 5:

(i) Strength decreased as particle size increased.

(ii) In the coarse dispersions, such as Material A, the deterioration of strength was less with increase of irradiation temperature.

(iii) In coarse and medium dispersions, loss of strength was greater as the burnup of heavy metal atoms increased, (compare Materials A with B, and C with D).

Examination of the matching fracture faces of a number of specimens showed that in all coarse and medium dispersions the fracture passed through the fuel particles, that is, the particles were still bonded to the matrix as in the pre-irradiation condition (Figure 5).

4. DISCUSSION

4.1 Types of Damage

Damage in dispersion fuels can arise from several sources:

(i) Fast Neutron Bombardment: In BeO this causes anisotropic lattice growth which decreases with increasing temperature and at temperatures up to 600–700 °C the macroscopic growth is equal to the lattice growth.

(ii) β–Particle Bombardment: A considerable flux of β–particles is present in fuel materials under irradiation arising from both the fission process and decay of fission products. This method of damage is usually neglected when considering damage in dispersion fuels, but in recent experiments by Walker and Hickman (1967), pieces of beryllia were separated from a slab of UO_2 by means of an aluminium foil, and the whole sandwich irradiated in a fast neutron flux. The aluminium retained the fission products that recoiled from the UO_2, but permitted the β particles to pass through to the beryllia. The results showed that the β flux caused an increase in the rate of anisotropic lattice growth beyond that due to fast neutron bombardment. X-ray measurements on the matrices of the coarse dispersions used in the present work were in accord with these findings (Table 4).

(iii) Fission Fragment Bombardment: This occurs uniformly throughout fine fuel dispersions if the interparticle distance is less than twice the fission fragment recoil range, but in coarse dispersions it is limited to a 15μ annulus around the fuel particles. The fuel particles are of course subjected to this type of damage. It is usually thought that the high energy of fission fragments causes this type of damage to be very severe. However, X-ray diffraction measurements on fuel materials (Walker and Hickman 1967) have shown that in BeO the lattice growth in fine fuel dispersions is negligible, that is, the fission fragments do not produce increased lattice growth and they anneal out the lattice growth produced by fast neutron irradiation. Walker and Hickman's experiments indicated that considerable macroscopic growth still occurred.

(iv) Fission Product Accumulation: Solid solution of fission products and formation of fission gas bubbles can cause damage in regions subjected to fission product bombardment.

In the light of these possible damage mechanisms we now consider the property changes of the fine fuel dispersions described earlier.

4.2 Behaviour of Fine Dispersions

Group 1 specimens were irradiated in a thermal flux with a very low ($< 10^{19}$ nvt) fast neutron dose, so the large observed volume changes cannot be due to fast neutron damage. Little or no lattice parameter changes were observed in these specimens so the volume changes cannot be due to β–particle bombardment as this produces a similar type of damage to that of fast neutrons. Swelling of fuel particles due to fission gas bubbles cannot explain the effect. In a separate experiment $(UTh)O_2$ with a uranium to thorium atom ratio of 1 to 10 was irradiated at 430–610 °C, and the observed swellings agreed well with the value of 1.5 per cent ΔV/at. per cent burnup established by Olsen et al. (1965). With two exceptions, the volume changes observed in Group 1 specimens are all too large to be attributed to the fuel particle swelling.

We conclude that the volume changes are due to defects produced by fission fragment bombardment – in these specimens the interparticle spacing was such that the whole sample was bombarded uniformly with fission fragments. The nature of the defect structure cannot be elucidated although as suggested by Walker and Hickman the lack of lattice parameter changes implies annealing

of the interstitial component of the damage and the macroscopic volume change must be due to accumulation of vacancy defects. This type of damage is observed in unfuelled BeO at temperatures in the region of 900–1100 °C, so fission fragment bombardment appears to produce at lower temperatures the same type of damage in unfuelled BeO as fast neutrons produce at higher temperatures.

In the fine dispersions, Group 2 specimens which contained 1.7 v/o of 5μ fuel particles were subjected to fast neutron, β particle and fission fragment bombardment. Reference to Table 3, Material E, shows that the observed volume changes exceeded those expected from fast neutrons alone (Pryor and Hickman 1966) by about 50 per cent. The X-ray diffraction measurements showed that the damage was similar to that of Group 1 specimens (i.e. no significant parameter changes) and quite different from that produced by fast neutron and β–particle bombardment. The swelling of the fuel particles would only have contributed about 0.13 per cent towards the overall swelling of the dispersions. Again it must be concluded that the volume changes were due to defects produced by fission fragment bombardment.

In Figure 6 the volume changes in fine dispersion specimens are plotted as a function of temperature and fission fragment flux. (In uniform dispersions the fission fragment flux is simply given by 2NR where N is the fission density and R is the fission fragment range). There is a reasonable correlation of volume change with fission fragment flux, and the volume change tends towards saturation at high doses and decreases with increasing temperature. These latter observations further confirm that the damage is due to defects, since annealing and hence reduced damage should occur both with increasing temperature and with increasing defect concentration. If the effect were due to fission gas swelling it should increase with temperature, and saturation effects should not be observed.

4.3 Behaviour of Coarse and Medium Dispersions

The situation is more complex for the coarse dispersions, where the fission fragment damage zones do not overlap; volume changes can occur in the intermediate matrix between the fuel particles and their recoil zones by fast neutron and β–particle bombardment. In addition volume changes in the annular recoil zone around the fuel particles, which is subjected to fission fragment bombardment, will occur by the same mechanism as in the fine fuel dispersions. As the volume of the region affected by this latter mechanism is small ($\sim$ 1 per cent) compared with the total volume, this latter effect would probably not contribute significantly to the total volume change; this view is confirmed by the good agreement obtained between X-ray and macroscopic growth figures. The volume changes of the coarse and medium dispersions given in Table 3 are compared with those expected from fast neutrons alone in Figure 7. The observed volume changes are, on average, about 25 per cent greater than expected, which is a measure of the additional growth caused by the simultaneous β flux. The effect does not appear to be very sensitive to temperature in the range 300–850 °C.

However in coarse dispersions, although 99 per cent of the matrix grows at the enhanced rate associated with neutron and β-particle bombardment, the annular recoil zones around the fuel particles grow at an even greater rate due to fission fragment bombardment. Their behaviour will almost certainly be of great importance in determining the mechanical strength of the irradiated dispersions. Their volume will increase at a greater rate than the surrounding beryllia matrix, internal stresses will build up in the dispersion and the strength will be reduced until macrocracks appear in the matrix. The change in strength of the coarse dispersions therefore depends on the strain developed between the matrix and the recoil zone. It should be noted that swelling of the fuel particle itself will not produce strains because the growth rate of the matrix exceeds that of the fuel particles. Only the recoil zone with the greater growth rate is important. The difference in mechanical behaviour of the coarse and intermediate dispersions can be explained on the basis of the recoil zone.

At a constant burnup the fission fragment flux in the recoil zone increases with increasing fuel particle size. This effect is illustrated in Figure 8 which gives the results of Monte Carlo calculations of the fission fragment flux as a function of a fuel particle size and distance from the fuel particles. At least in the inner region of the recoil zone the fission fragment flux is higher for 200μ particles than 50μ particles, and both are higher than a uniform fine dispersion.

If the above argument is correct, then, since it was shown earlier that the volume change increases with increasing fission fragment flux, the strength after irradiation should correlate with the fission fragment flux in the recoil zone. In Figure 9 the percentage strength remaining in the coarse dispersions is plotted as a function of fission fragment flux at the surface of the fuel particles. There is an obvious trend of decreasing strength with increasing fission fragment dose. Note also that the loss of strength at a given dose decreases with increasing temperature owing to the decreasing volume change in the annulus.

4.4 Application to Fuel Element Design

Previous work on unirradiated dispersions (Veevers and Rotsey 1966a and 1966b) showed that if the fuel particle size did not exceed 5μ (the size of a critical crack in the beryllia matrix) the strength of the dispersion was not significantly less than that of pure beryllia. Larger fuel particle sizes caused greater losses in strength.

The present results show that fine fuel dispersions also have the best resistance to irradiation if the interparticle spacing is less than twice the recoil distance of fission fragments, that is, 30μ, ensuring uniform damage throughout. Thus fine fuel dispersions appear to be the best choice.

However, fuel element design should take into account the difference in the volume changes caused by different types of damage. For example, Christie et al. (1964) and Roberts (1964) proposed designs in which the dispersion was coated with a fuel free beryllia layer in order to retain fission products. We can now see that although fine dispersions are the best choice of materials, they are not the best choice in such a fuel element design. The fission fragment bombardment in the dispersion will cause much greater volume changes than the fast neutron dose will cause in the beryllia coating, and after quite a short irradiation at, say, 500 °C the core will burst open the shell.

If the dispersion is made from coarse fuel particles, then the growth rate from neutrons plus β particles is less than that from fission fragments, but still exceeds the growth rate of the coating which receives only fast neutrons. In this case it may be preferable to reduce the coating thickness to 0.030 in. (half the range of a β particle in BeO) so that the coating grows at a similar rate to the core. Unfortunately the strength of the core will diminish as irradiation proceeds as shown earlier by the results of mechanical tests on coarse dispersions.

Possible solutions to the problems of fuel element design lie in the direction of high operating temperatures or separation of the core from the shell so that strains are not transmitted from one to the other.

5. CONCLUSIONS

1. When fine dispersions are irradiated in a fast neutron flux, fission fragment damage is the prime cause of volume increases. The volume changes increase with increasing fission fragment flux and decrease with increasing temperatures. The lattice parameters of the beryllia matrix are not significantly altered, yet the volume changes are much greater than those caused by fast neutron damage.

2. When coarse or medium dispersions are irradiated in a fast neutron flux the simultaneous β flux from the fuel particles causes increased anisotropic lattice growth in the beryllia matrix. The volume changes, though less than those caused by fission fragments, are larger than those caused by fast neutrons alone. Thus, when the interparticle spacing in dispersions exceeds twice the recoil distance (30 μ) irradiation causes differential macrogrowth within the dispersion. Owing to fission fragment bombardment the recoil zones grow faster than the matrix, under fast neutron and β particle bombardment. The resultant internal stresses reduce the strength. The loss of strength increases as fuel particle size and burnup increases, but decreases as irradiation temperatures increase.

3. Maximum initial strength and maximum retention of strength under irradiation can be achieved by using particles less than 5μ, spaced not more than 30μ apart.

6. ACKNOWLEDGEMENTS

The assistance of Dr. D.G. Walker in providing the Monte Carlo solutions, and for many helpful discussions is gratefully acknowledged. Thanks are due to the Ceramics Group for fabrication of the specimens, to the Hot Cells Group for post irradiation measurements, and to Mr. J. McCracken for the metallography.

7. REFERENCES

Christie, G.E., Jackson, J., Lyons, G.A., Cragg, D.C., and Martin, F.S. (1964). – Journal Nucl. Mat., 14: 444–452.

Hamner, R.L., Chapman, A.T., and Harms, W.O. (1964). – Journal Nucl. Mat. 14: 465–472.

Hanna, G.L., and Hilditch, R.J. (1965). – AAEC/E140.

Hanna, G.L., Hilditch, R.J., Hickman, B.S. (1964). – Journal Nucl. Mat., 14: 473–481.

Hilditch, R.J., Hickman, B.S., Rotsey, W.B., and Veevers, K. (1966). – Journal Nucl. Mat., 20: 119–121

Mills, R.G., Barnes, J.O., Johnson, D.E., and Simnad, M.T. (1964). – Journal Nucl. Mat., 14: 482–486.

Olsen, A.R., Douglas, D.A., Hirose, Y., Scott, J.L., and Ullmann, J.W. (1965). – ORNL–P–1724.

Pryor, A.W., and Hickman, B.S. (1966). – AAEC/TM318.

Roberts, W.H. (1964). – Journal Nucl. Mat., 14: 14–40.

Rotsey, W.B., McDonald, N.R., and Veevers, K. (1967). – Proceedings of Brit. Ceram. Soc., 7: 205–219.

Veevers, K., and Rotsey, W.B. (1966a). – AAEC/TM338.

Veevers, K., and Rotsey, W.B. (1966b). – Journal of Materials Science, 1: 346–353.

Walker, D.G., and Hickman, B.S. (1967). – Journal Nucl. Mat., 24.

TABLE 1

TYPES OF MATERIAL IRRADIATED

Identification of Material	Volume Per cent of $(UTh)O_2$ in BeO	U/Th Ratio and State	Fuel Particle Size Microns	Classification of Dispersion
A	1.7	1 : 10 Solid Solution	150–200	Coarse
B	1.7	1 : 10 as 1 : 5 Solid Solution + 5 Free Thoria	150–200	Coarse
C	1.7	1 : 10 Solid Solution	30–50	Medium
D	1.1	2 : 6 Solid Solution	30–50	Medium
E	1.7	1 : 10 Solid Solution	< 5	Fine
F	5	2 : 3 Solid Solution	<10	Fine
G	15	2 : 3 Solid Solution	<10	Fine
H	15	3 : 1 Solid Solution	<10	Fine
J	25	2 : 3 Solid Solution	<10	Fine

TABLE 2

GROUP 1 FUEL DISPERSIONS, IRRADIATION CONDITIONS AND VOLUME CHANGES

Material			Mean Irradiation Temperature °C	Mean Thermal Neutron Dose nvt	Mean per cent Burnup of Heavy Metal Atoms	Mean per cent Volume Change
Code	U/Th	Vol.%				
F	2 : 3	5	760 770	4.29×10^{20} 2.24×10^{19}	8.4 3.7	2.18 1.38
G	2 : 3	15	500 540 800 875 880 900 900	1.85×10^{20} 2.68×10^{20} 3.63×10^{20} 2.1×10^{20} 2.98×10^{20} 2.07×10^{20} 2.46×10^{20}	2.5 5.7 7.4 2.8 6.3 2.6 3.3	2.54 2.9 1.4 1.19 2.2 1.35 1.86
H	3 : 1	15	750	2.44×10^{20}	5.4	2.06
J	2 : 3	25	790 800	2.78×10^{20} 2.3×10^{20}	5.9 2.5	1.7 1.57

TABLE 3

GROUP 2 FUEL DISPERSIONS, IRRADIATION CONDITIONS AND VOLUME CHANGES

Material			Mean Irradiation Temperature °C	Mean Fast Neutron Dose nvt x 10^{20} (> 1 MeV)	Mean Per cent Burnup of Heavy Metal Atoms	Mean Per cent Volume Change Observed	Mean Per cent Volume Change Expected from Fast Neutrons
Code	U/Th	Vol.%					
A Coarse	1:10	1.7	300	3.6	4.7	1.75	1.18
			510	4.0	5.0	0.83	0.78
			610	4.5	5.4	0.90	0.60
			675	3.6	5.0	0.47	0.43
			775	3.9	5.3	0.68	0.38
			850	4.7	5.7	0.64	0.42
B Coarse	1:10 overall	1.7	675	3.6	8.6	0.52	0.43
			775	3.9	9.3	0.54	0.38
			850	4.7	9.6	0.55	0.42
C Medium	1:10	1.7	300	3.6	4.7	1.53	1.18
			510	4.0	5.0	0.97	0.78
			610	4.5	5.4	0.87	0.60
D Medium	2:6	1.1	300	3.6	12.3	1.84	1.18
			510	4.0	12.9	1.11	0.78
			610	4.5	13.9	0.90	0.60
E Fine	1:10	1.7	300	3.6	4.7	1.77	1.18
			510	4.0	5.0	1.18	0.78
			610	4.5	5.4	0.97	0.60

TABLE 4

LATTICE PARAMETER CHANGES OF BERYLLIA IN COARSE FUEL DISPERSIONS AND IN UNFUELLED BERYLLIA

Material	Fast Neutron Dose nvt x 10^{20}	Mean Irradiation Temperature °C	Lattice Parameter Change Per Cent	
			$\frac{\Delta c}{c}$	$\frac{\Delta a}{a}$
A	2.5	675	0.46	0.04
BeO	2.5	675	0.33	0.04
B	2.5	675	0.46	0.03
A	3.2	775	0.36	0.01
BeO	3.2	775	0.21	0.02
B	3.2	775	0.39	0.02

TABLE 5

RESULTS OF MODULUS OF RUPTURE TESTS ON FUEL DISPERSIONS

Material	Fuel Particle Size – Microns	Per cent Burnup of Heavy Metal Atoms	Mean Irradiation Temperature °C	Modulus of Rupture (10^3 p.s.i.) over 20–500 °C		Percentage Strength Remaining	Number of Specimens Irradiated
				Pre–Irradiation	Post–Irradiation		
A	150 – 200	4.7	300	20.0	5.2	26.0	30
		5.0	510	20.0	7.3	36.5	30
		5.4	610	20.0	7.7	38.4	29
		5.0	675	17.0	8.9	52.3	20
		6.3	775	17.0	9.7	57.0	20
		5.7	850	17.0	11.8	69.0	20
B	150 – 200	8.6	675	17.8	7.8	43.8	20
		9.3	775	17.8	8.7	49.0	20
		9.6	850	17.8	10.6	59.5	20
C	30 – 50	4.7	300	24.5	13.4	54.8	30
		5.0	510	24.5	14.3	58.3	30
		5.4	610	24.5	12.2	48.8	29
D	30 – 50	12.3	300	24.0	8.7	36.2	10
		12.9	510	24.0	11.3	47.0	10
		13.9	610	24.0	8.4	35.0	8
E	<5	4.7	300	24.5	22.7	93.0	30
		5.0	510	24.5	18.6	86.0	30
		5.4	610	24.5	18.2	84.0	29

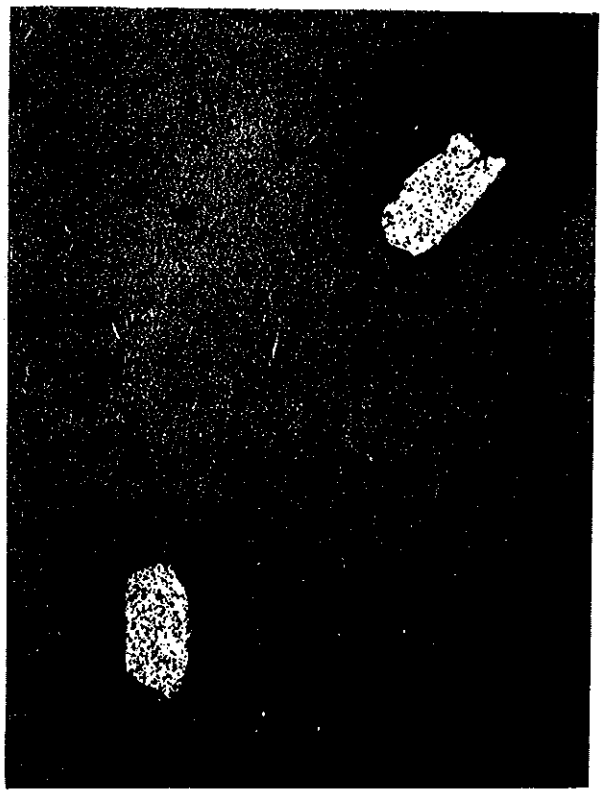

X75

1.7 VOL. % $(UTh)O_2$ 200μ

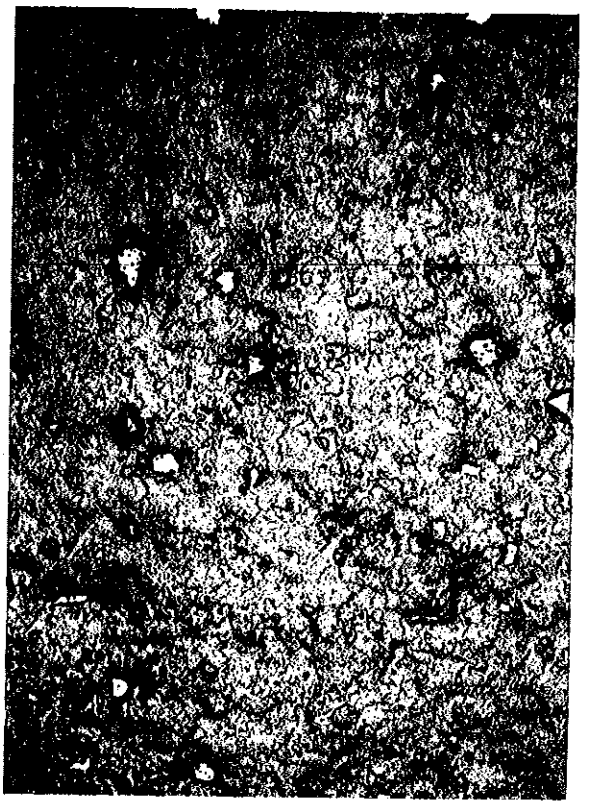

X75

1.7 VOL. % $(UTh)O_2$ 50μ

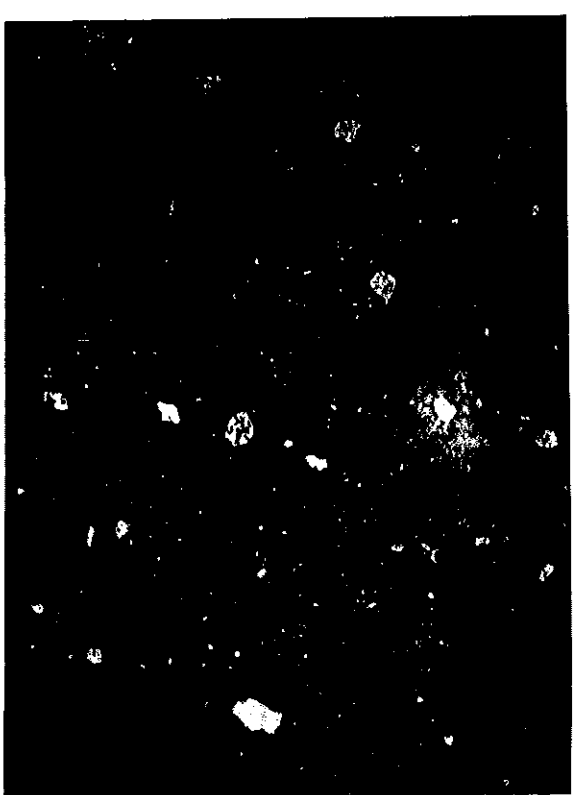

X500

1.7 VOL. % $(UTh)O_2 < 5\mu$

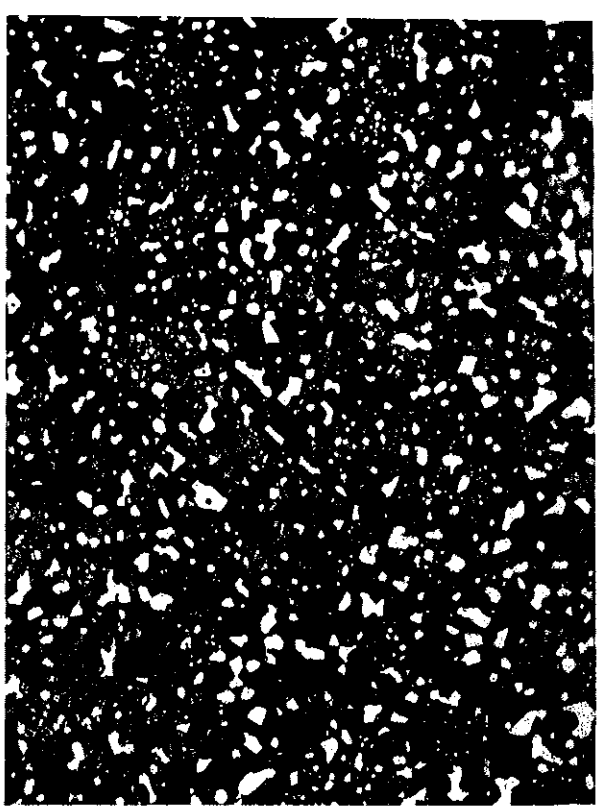

X500

15 VOL. % $(UTh)O_2 < 10\mu$

FIGURE 1. TYPICAL MICROSTRUCTURES OF DISPERSIONS

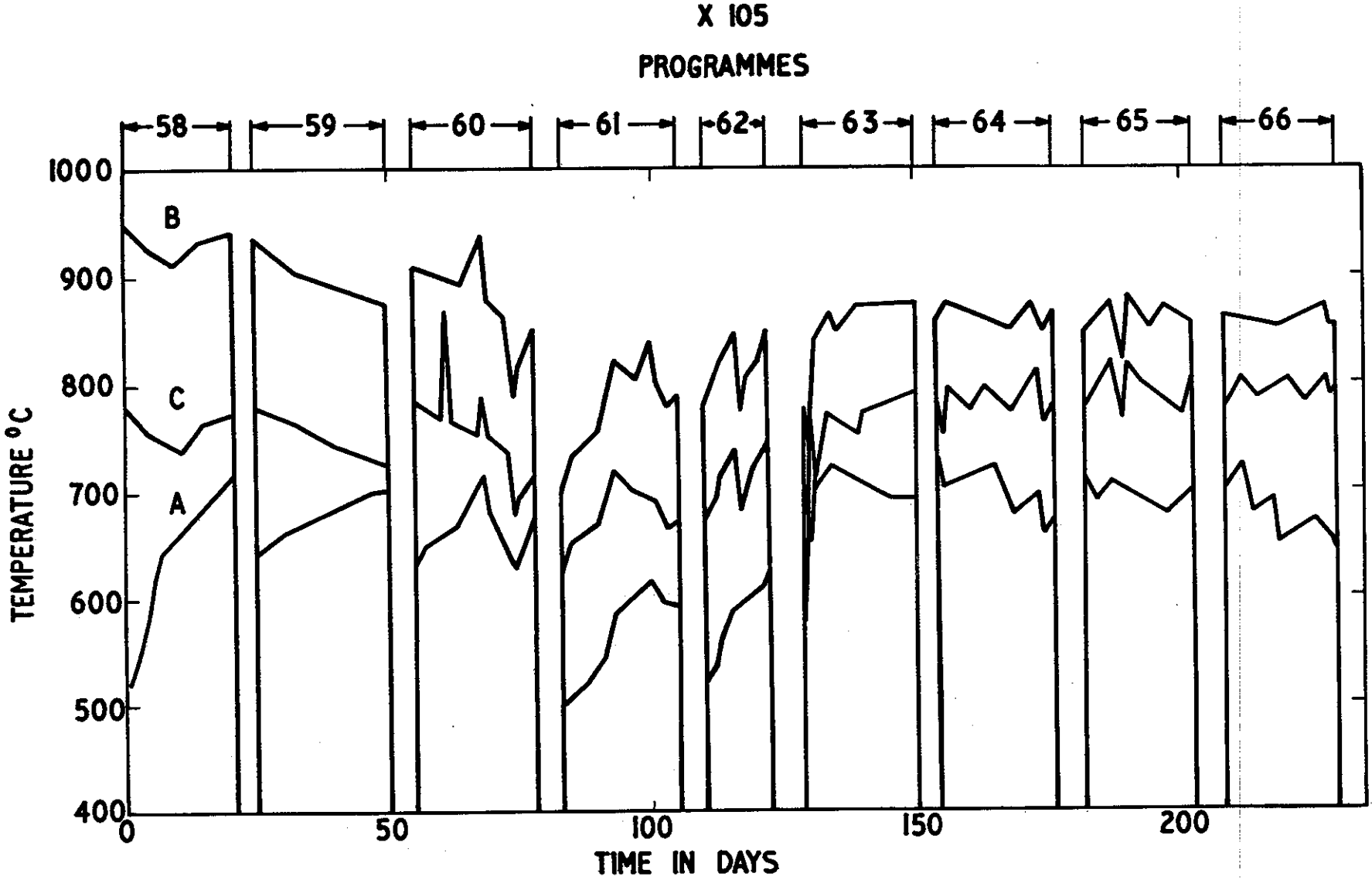

FIGURE 2. TYPICAL TEMPERATURE HISTORY OF IRRADIATION RIG

P1109

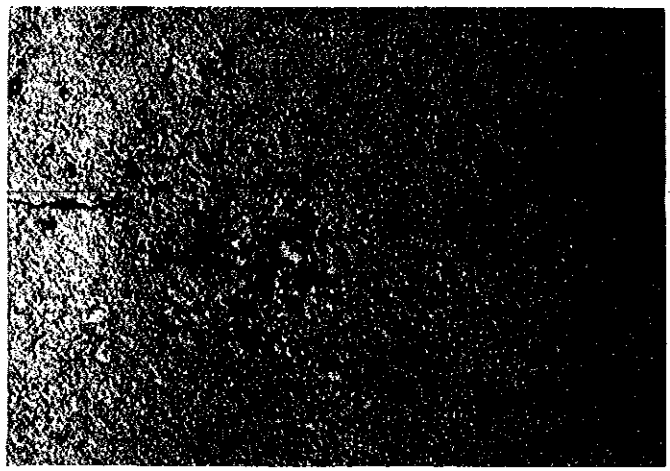

X67

200μ DISPERSION 510°C IRRADIATION
TEMPERATURE 4 at. % BURNUP

FIGURE 3. MACROCRACKS IN IRRADIATED COARSE FUEL DISPERSIONS

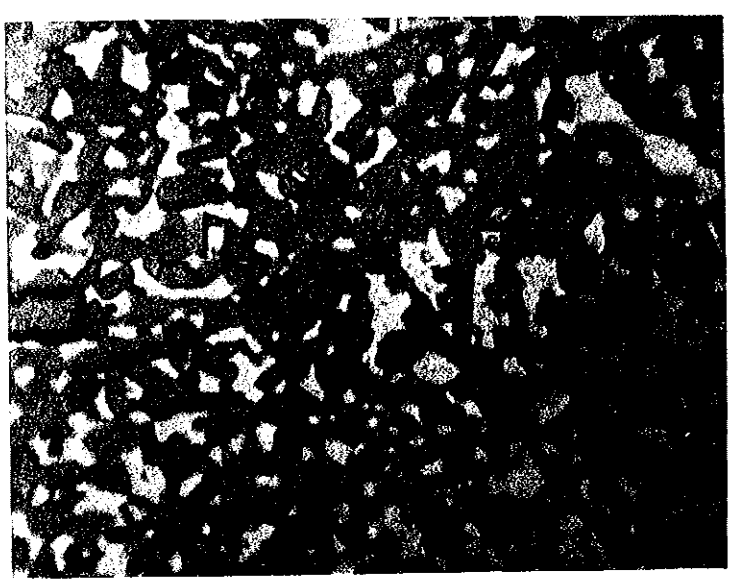

a) UNIRRADIATED X1030

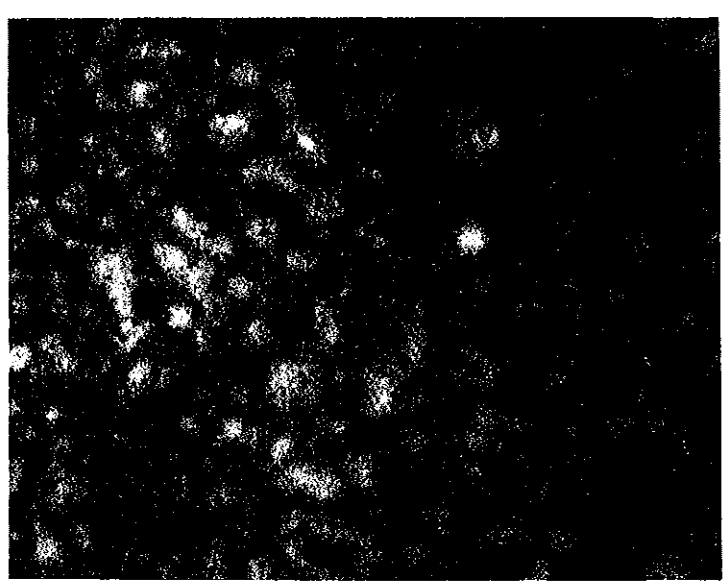

b) IRRADIATED X1030

15 VOL. % $(UTh)O_2$ <10μ DISPERSION

FIGURE 4. DIFFUSE FUEL-MATRIX BOUNDARIES

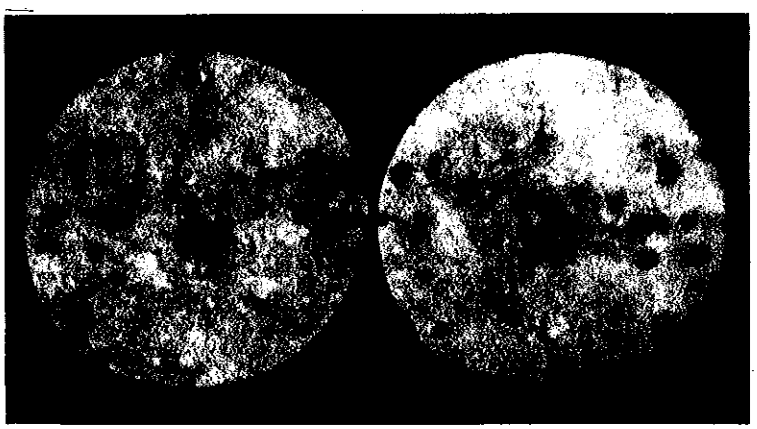

X10

FIGURE 5. MATCHING FRACTURE FACES IN 200μ DISPERSION AFTER IRRADIATION

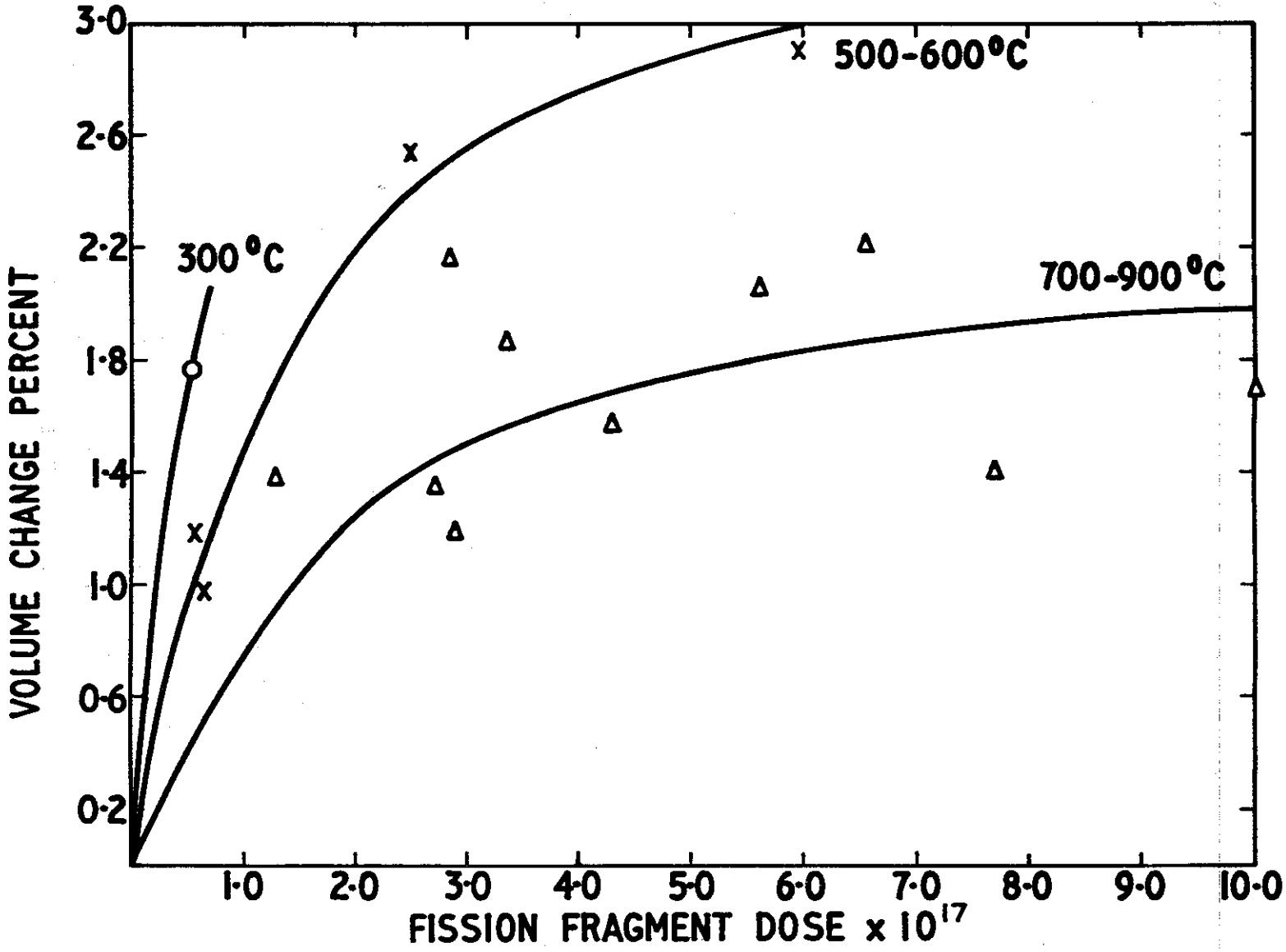

FIGURE 6. VOLUME CHANGE v. FISSION FRAGMENT DOSE FOR FINE FUEL DISPERSIONS

P1109

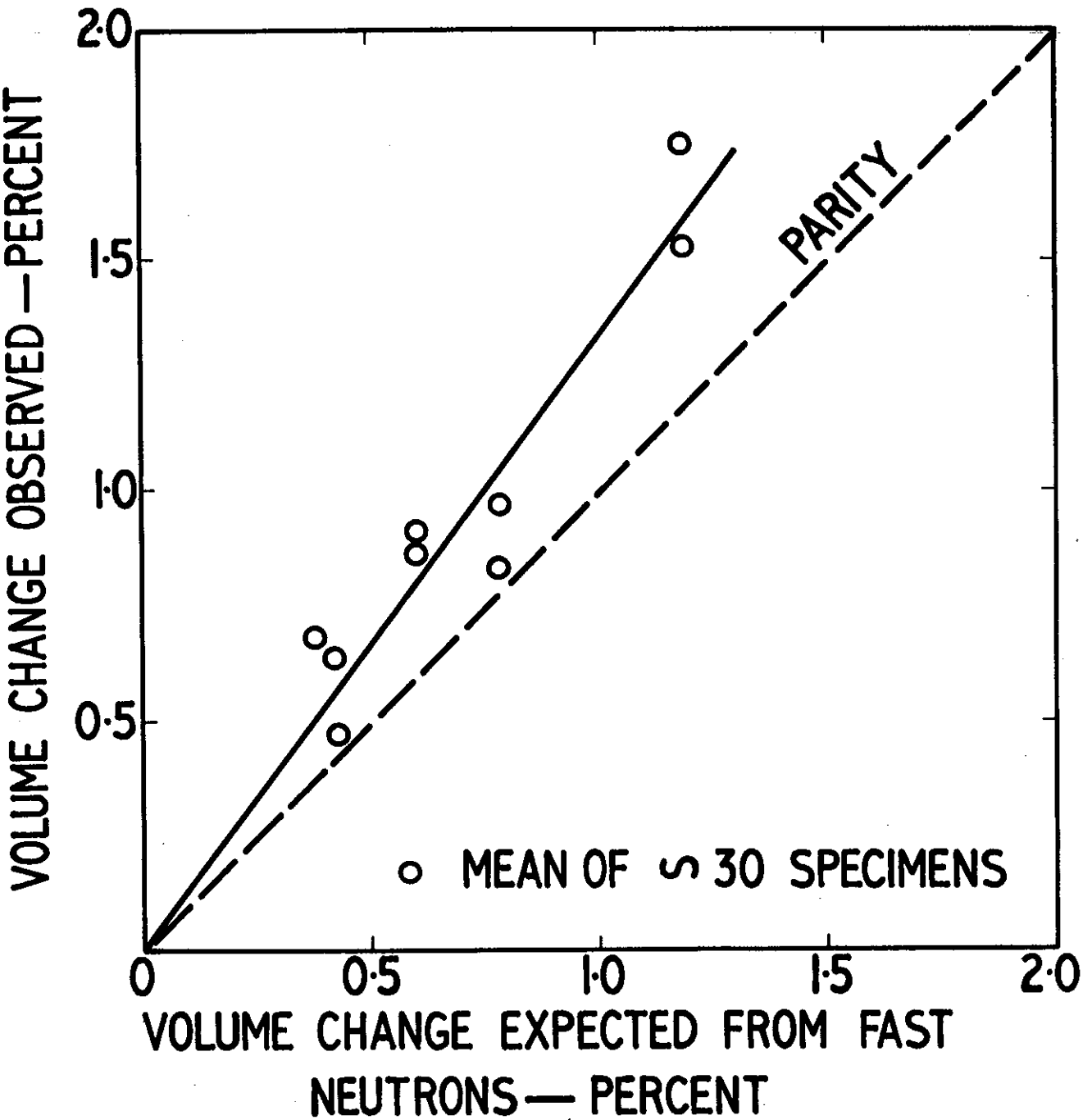

FIGURE 7. VOLUME CHANGES IN COARSE AND MEDIUM FUEL DISPERSIONS AFTER ~5 at. % BURNUP

P1109

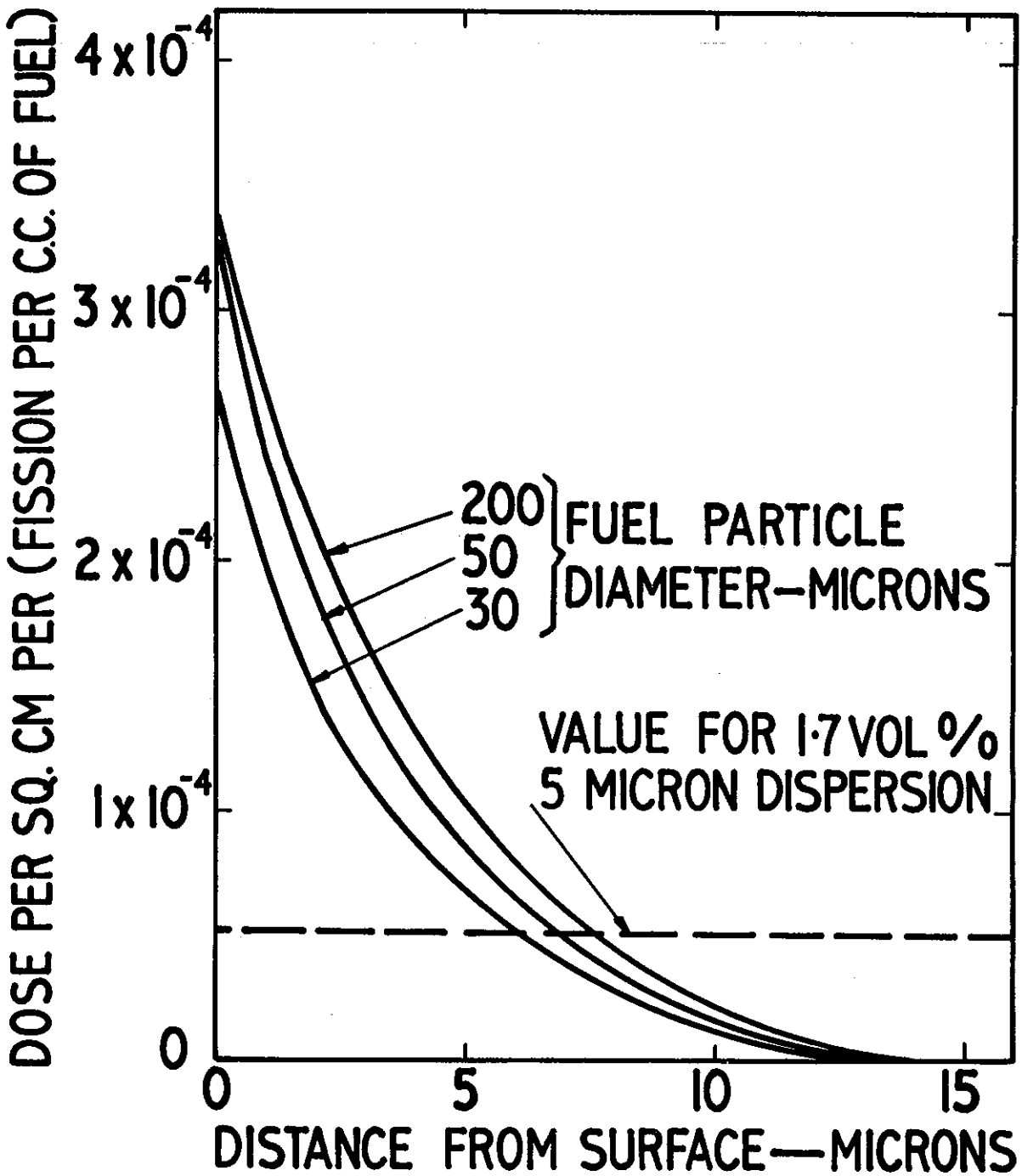

FIGURE 8. COMPARISON OF FISSION FRAGMENT FLUX OF COARSE AND MEDIUM FUEL DISPERSIONS WITH FINE DISPERSIONS

P1109

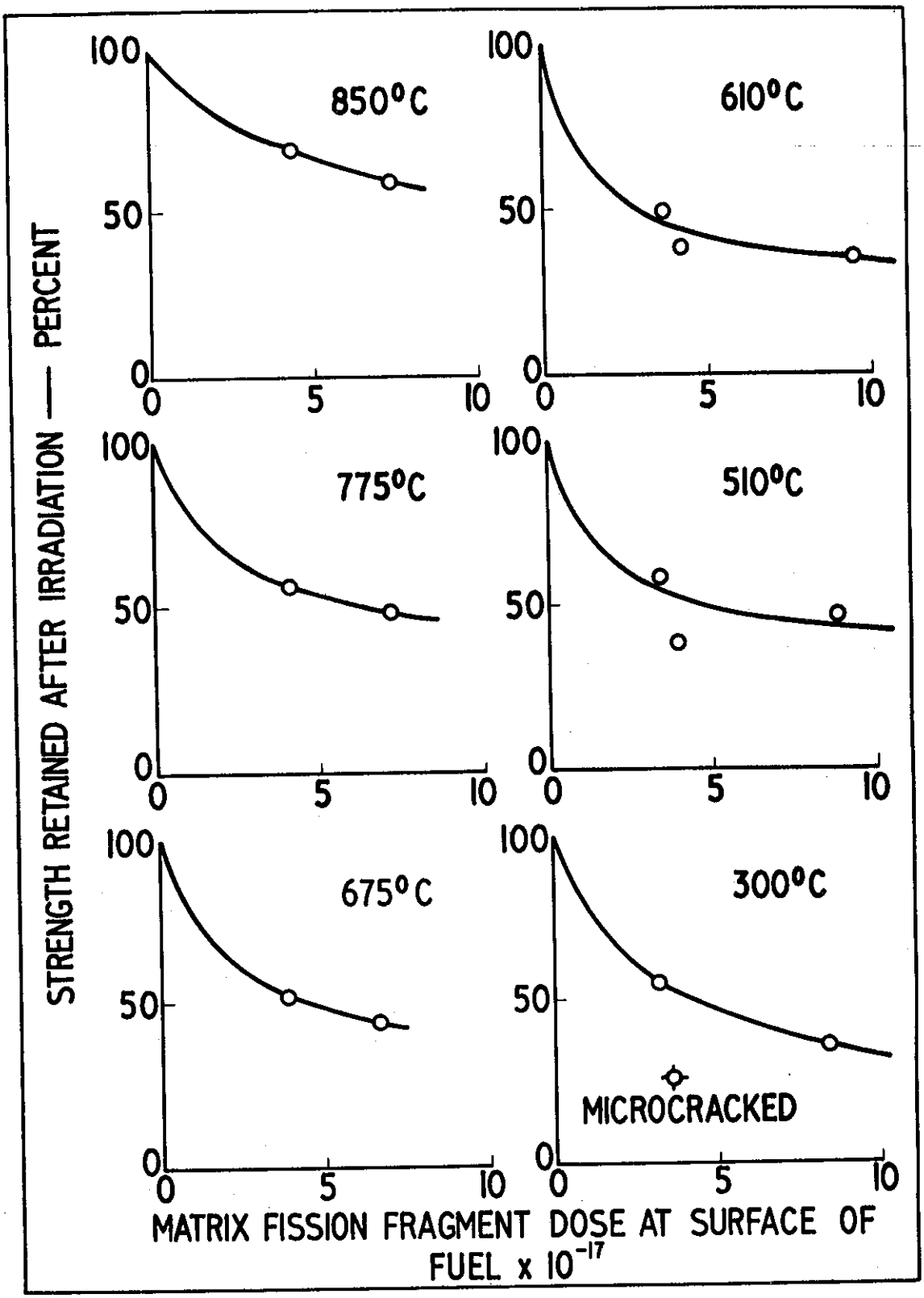

FIGURE 9. RETAINED STRENGTH v. FISSION FRAGMENT DOSE AT SURFACE OF FUEL FOR COARSE AND MEDIUM DISPERSIONS

P1109